^{7}Li and ^{6}Li magic angle spinning NMR studies of two types of metallic Li colloids formed by electron irradiation in LiF

O. J. Żogał*
Institute of Low-Temperature and Structure Research, Polish Academy of Sciences, PL-50950 Wrocław, Poland

F. Beuneu and P. Vajda
Laboratoire des Solides Irradiés, École Polytechnique, F-91128 Palaiseau, France

P. Florian and D. Massiot
Centre de Recherches sur la Physique des Hautes Températures, CNRS, F-45071 Orléans, France
(Received 4 February 2002; published 1 August 2002)

The ^{6}Li and ^{7}Li magic angle spinning NMR spectra of 2.5-MeV electron-irradiated LiF crystals have been measured in a field of 9.4 T. Two samples which had received doses of 1.17 C/cm^2 [low dose (LD)] and 2.33 C/cm^2 [high dose (HD)] were studied. Besides the resonance line of the ionic compound, a second well-separated spectrum is observed which lies in the region of the Knight shift value for metallic lithium. At room temperature, the latter can be decomposed into two components with different Knight shift and linewidth values. For the LD sample, they are located at 271.7 ppm and 264.3 ppm with 1600 and 610 Hz widths, respectively. In the HD specimen, the positions and linewidths are 267.2 and 264.3 ppm and 2580 and 470 Hz, with a much larger contribution of the broad component to the total intensity. When the temperature is increased line narrowing takes place at first, indicating a shortening of correlation times for self-diffusion, practically independently in both components. Above roughly 373 K, both lines broaden and approach each other before collapsing into a single line caused by exchange between the two sets. We attribute the higher-ppm component to metallic lithium under higher than atmospheric pressure, while the other corresponds to Li under normal conditions. The thermal evolution of the spectra indicates that annealing processes take place during heat treatment, with partial transformation of the ''high-pressure'' lithium into normal metal. The former disappears completely after crossing the melting temperature of metallic lithium (454 K), due to stress relaxation. Simultaneously, the Knight-shifted spectrum moves towards lower ppm values, reducing the separation from the central ionic line by nearly 4 ppm at the Li melting point.

DOI: 10.1103/PhysRevB.66.064101 PACS number(s): 61.72.Ji, 76.60.Cq, 61.80.Fe, 82.70.Dd

I. INTRODUCTION

The investigation of radiation damage in lithium compounds (Li_2O, LiF) is of high interest from a basic point of view (the physics of point defects and their clusters) and for their potential application in nuclear fusion reactors. Several experimental techniques for the study of their properties have been used already. The conduction electron spin resonance[1,2] (CESR), ^{7}Li-nuclear magnetic resonance[1,3–7] (NMR), and differential scanning calorimetry[8] are among others. Optical studies of neutron-irradiated[9] and ion-implanted[10] LiF permitted one to follow the transformation of color centers into larger clusters and eventually into colloids. It was shown[11] that NMR is especially well suited for examining the microscopic properties of solids. In particular, metallic Li colloids can be easily detected by ^{6}Li and ^{7}Li NMR because of their relatively large Knight shifts in comparison to very small chemical shift interactions in lithium compounds. Therefore, the ''metallic'' signals can be well separated from the ionic matrix using a large magnetic field. In addition, the fast diffusive motion of lithium in metal precipitates, which occurs at room temperature and above, averages out—to a large extent—the dipolar interaction. Thus, the absorption lines of ^{7}Li become narrow. The above NMR analytical properties can be still enhanced by using the magic angle spinning (MAS) technique. Rapidly spinning the sample at an angle of 54.70° to the applied magnetic field removes the line broadening resulting from such interactions as incompletely averaged (due to atomic motion) dipolar interaction, chemical shift anisotropy, first-order quadrupole interaction, and magnetic susceptibility effects if they are present. As an effect, better resolution than in static spectra is expected.[11] Besides from the most popular ^{7}Li NMR, additional information can be gained from NMR investigations using the ^{6}Li isotope. Although the natural abundance of the ^{6}Li isotope is more than 10 times smaller than of ^{7}Li, resulting in much lower sensitivity, other characteristics, such as the dipolar and quadrupolar interactions (the electric quadrupolar moment of ^{6}Li is more than 60 times smaller), are very different from those of ^{7}Li. Therefore, complementary studies by ^{6}Li NMR seemed advisable.

In this work, we report ^{7}Li and ^{6}Li NMR studies in two irradiated single-crystal samples of LiF at elevated temperatures, using MAS-NMR on both isotopes.

Using this technique allowed us to detect a more complex structure of the spectrum than until now observed in conventional static experiments. In particular, changes in spectral shape appear clearly during temperature variation. To the authors' knowledge, the kind of experiments reported here has never been published before.

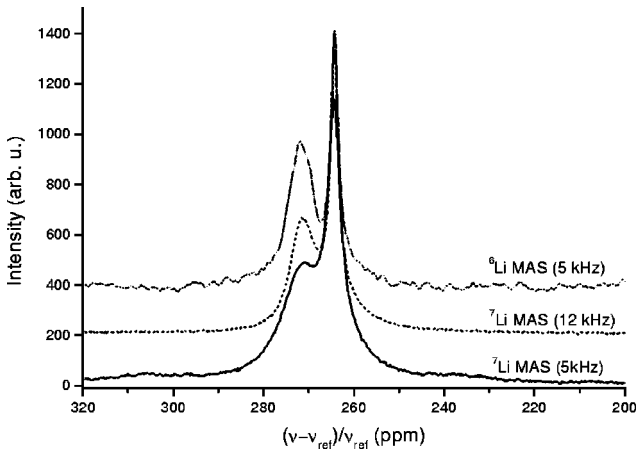

FIG. 1. ^{7}Li and ^{6}Li MAS NMR spectra for the low-dose irradiated (LD) sample taken at room temperature with 64 and 58 800 acquisitions, respectively. The MAS rotor frequencies are noted in the brackets (the base lines of the spectra have been shifted, for the sake of clarity).

II. EXPERIMENTAL DETAILS

The samples have been uniformly irradiated by 2.5-MeV electrons from a Van de Graaff accelerator, with a current of the order of 15 μA/cm^2. During electron bombardment, they were fixed on a water-cooled copper target with a 10-μm-thick copper foil. The irradiation temperature, monitored by a thermocouple, was about 50 °C. Two fluences were employed: 2.33 C/cm^2 [high-dose (HD) sample] and 1.17 C/cm^2 [low-dose (LD) sample]. The initially bulk plateletlike crystals were broken up into below-mm-size grains [which remained monocrystalline and (100) oriented] after irradiation, indicating a serious swelling effect.

The ^{7}Li and ^{6}Li MAS NMR spectra were obtained on a Bruker DSX 400 spectrometer (9.4 T) operating at 155.5 and at 58.9 MHz, respectively, and frequency referenced to an external 1-mol LiCl aqueous solution. In most cases, a Hahn echo sequence ($\pi/2$-τ-π-τ-acquire) was used before Fourier-transformed spectra were recorded. The spectrum consists of a wide and a narrow line. The wide signal corresponds to ^{7}Li or ^{6}Li nuclei in the ionic LiF lattice and is out of scope of our interest here.

The radio frequency pulses were strong enough to irradiate the entire ''metallic'' spectrum. MAS spectra were obtained with spinning rates of 5 kHz, although, at room temperature, 12 kHz was also used with a standard 4-mm rotor. The temperature in the 293–490 K range was regulated using a standard controller provided with the spectrometer. Since the temperature readout outside of the rotor differs from the temperature inside the sample, calibration was made using $Pb(NO_3)_2$ as described by Takashi *et al.*[12]

III. RESULTS AND DISCUSSION

A. Low-dose irradiated sample

Figure 1 presents the ^{7}Li and ^{6}Li NMR spectra under MAS conditions for the LD sample (less irradiated) taken at room temperature. In contrast to earlier NMR studies,[3] where the metallic contribution was observed as a single line, a two-component structure of the spectra is seen. The structure is more developed for the 12-kHz spinning rate than for 5 kHz. However, the positions of the two lines are the same for both spectra, within experimental error. In addition, the result of the ^{6}Li MAS NMR measurements is shown in Fig. 1, too. This experiment is much more demanding, because the signal is about 400 times less intense than that of ^{7}Li . However, it offers an even better resolution since quadrupolar and dipolar interactions are weaker than for ^{7}Li nuclei. The second moment of the ''rigid'' lattice, M_2, calculated for the ^{6}Li nucleus from Van Vleck's[13] formula, (with a lattice constant for Li of 3.5092 Å), yielding the dipolar interaction, is equal to 0.7 kHz^2 while for the ^{7}Li it is 10.7 kHz^2. Comparison of the positions for the two lines in the ^{7}Li and the ^{6}Li spectra indicates that they are again the same within experimental error. The shape of the lines can be described, to a good approximation, by a Lorentzian function. Their linewidths, full width at half maximum (FWHM), are given in Table I. The presented data can be related to NMR data reported earlier for metallic lithium. A Knight shift equal to 260 (2) ppm is given for lithium by Carter *et al.*[14] in their review of metallic shifts in NMR. In our work, one of the two observed lines, at 264 ppm, is very close to the value cited above. As expected, the linewidths given in Table I are much smaller than calculated from Van Vleck's formula, since the self-diffusion process has been shown[15] to occur already at room temperature in lithium metal. The process averages out the dipolar interaction to a large extent, thus narrowing the resonance lines. In addition, MAS-NMR reduces the linewidth $\Delta\nu_{1/2}$ according to following approximate formula[16]:

$$\Delta\nu_{1/2}=\frac{1}{3}M_2\left[\frac{2\tau_c}{1+(\nu_r\tau_c)^2}+\frac{\tau_c}{1+4(\nu_r\tau_c)^2}\right], \qquad (1)$$

where ν_r and τ_c are the rotation frequency and the correlation time of the dipolar interaction. If one takes the above calculated M_2 of ^{7}Li and $\tau_c(296\ \mathrm{K})=5.9\times10^{-6}$ sec, one obtains a value of $\Delta\nu_{1/2}=63$ Hz. Here, the correlation time used is that calculated from the NMR data for metallic lithium.[15] On the other hand, NMR studies of sodium col-

TABLE I. Decomposition of the spectra of the LD sample shown in Fig. 1 into two Lorentzian components. Uncertainties in the line positions are ±0.3 ppm and ±0.6 ppm for the low and high value shifts, respectively. They are $\pm7\%$ for the linewidths.

Nucleus	MAS (kHz)	Line position (ppm)	Linewidths (Hz)
^{7}Li	5	271.8	1600
		264.3	610
^{7}Li	12	271.2	1010
		264.3	383
^{6}Li	5	271.7	370
		264.2	116

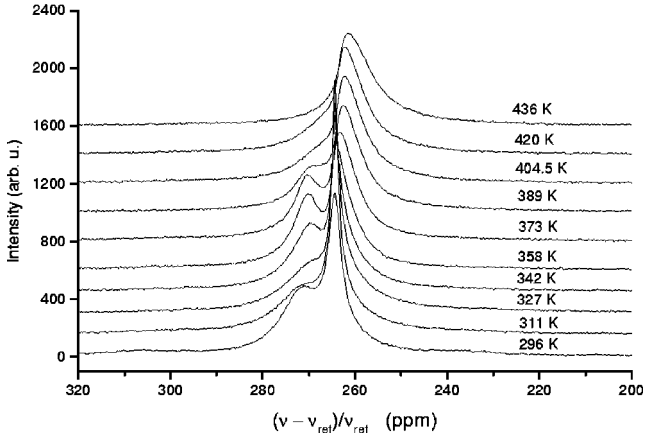

FIG. 2. Thermal evolution of the ^{7}Li MAS (5 kHz) NMR spectra of the LD sample, during the first heating run.

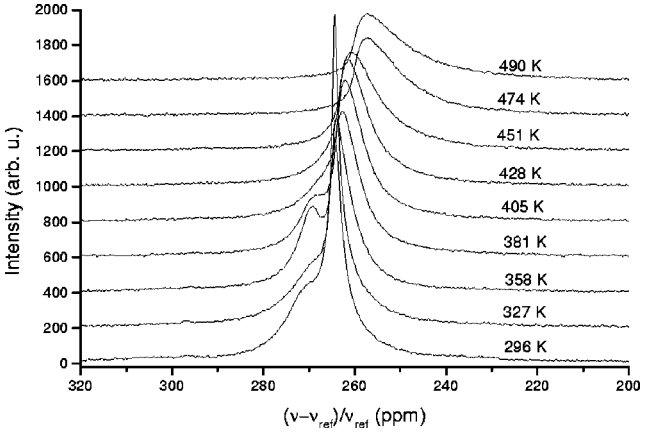

FIG. 3. Thermal evolution of the ^{7}Li MAS (5 kHz) NMR in the LD sample in the second heating run, where the melting point (454 K) of metallic lithium was crossed.

loids in heavily irradiated NaCl (Ref. 17) indicated a longer correlation time than for bulk metallic sodium. Thus, when, for example, a $\tau_c(296\ \mathrm{K}) = 5.9\times10^{-5}$ sec is used we obtain a $\Delta\nu_{1/2} = 350$ Hz which is close to the experimental values of the narrower line shown in Table I. Therefore, we may identify the narrower signal (near 264 ppm) as originating from lithium in an environment close to normal bulk metal.

The second, broad, signal (near 271 ppm) could originate from a high-pressure phase, as, e.g., observed by Bertani *et al.*[18] in NMR measurements of bulk lithium under pressure. These authors report a displacement of the ^{7}Li Knight-shift signal toward higher values and inhibition of translational diffusion with increasing pressure, at room temperature. Rough estimates (read from their Figs. 2 and 3) of the changes, for pressures of the order of 2 GPa, yield a shift by 6 ppm upwards with respect to ambient pressure and a lower value of the self-diffusion coefficient (and, consequently, a lower value of the correlation time and a broader absorption line) by a factor of 3. So this kind of change could account for the observed features of the broader component of the ^{7}Li signal located at 271 ppm in Fig. 1.

The observation of two kinds of lithium colloids created by irradiation of lithium compounds was already published in the past: Lambert and Guinier[19] identified fcc and bcc lithium in neutron-irradiated LiF by x-ray scattering and noticed that fcc Li disappears when LiF is heated through the melting point of Li. More recently, we observed by electron spin resonance (ESR) the presence of two types of metallic Li precipitates[1,2] in electron-irradiated Li_2O: small colloids of unknown structure and much larger ones, made of bcc Li, in the close neighborhood of large oxygen bubbles. In both cases, a general picture can be the following: at the beginning of irradiation damage, nonmetallic ions are taken off and metallic precipitates are nucleated, in epitaxy with the (insulating) host matrix. This was proved in the LiF case,[19] where the fcc Li network is indeed in epitaxy with the fcc lattice of LiF, and it is an interesting possibility for Li_2O, where the small colloids could be simple cubic Li in epitaxy with the Li sublattice of the oxide. Increasing the irradiation fluence and/or performing some annealing induces growing of the precipitates, preferentially near cracks or gas bubbles where the stresses are reduced, giving rise to normal bcc lithium. The swelling described in the experimental section, which leads to sample breakup during irradiation, is a strong indicator in favor of this model. It is interesting that the swelling reported in heavy-ion irradiated LiF by Trautmann *et al.*[20] was attributed by them to defect aggregates such as Li colloids connected to fluorine and/or vacancy clusters: an analogous configurational image.

Thus, it is reasonable to imagine for our present experimental conditions the presence of two types of metallic Li colloids. The first type, probably of small size, comes from the initially fcc Li and, due to the fact that the Li sublattice in LiF is denser than normal bcc Li, finds itself under pressure. A rapid estimate—using the Li-sublattice parameter of $a^{\mathrm{Li}}_{\mathrm{fcc}} = 4.01$ Å and comparing with the bulk value $a^{\mathrm{Li}}_{\mathrm{bcc}} = 3.51$ Å—yields a volume increase of $(\Delta V/V)_{\mathrm{Li}} \sim 0.34$ per Li atom for the latter which results, when applying a bulk modulus of $B_{\mathrm{Li}} = (\Delta P/\Delta V)V_{\mathrm{Li}} = 11.5$ GPa, in a

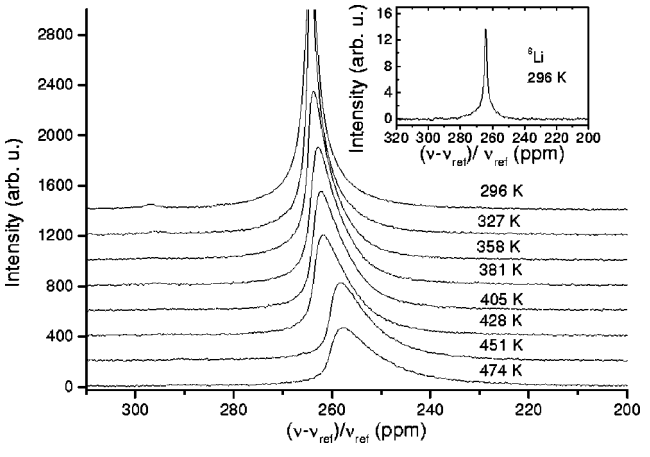

FIG. 4. Thermal evolution of the ^{7}Li MAS (5 kHz) NMR in the LD sample during cooling from 490 K to 296 K. The inset shows the ^{6}Li MAS (5 kHz) NMR spectrum recorded at room temperature (296 K) after cooling from 490 K. The two-line structure observed in the earlier heating and cooling runs is lost.

pressure of $\Delta P \sim 4$ GPa: the same order of magnitude as estimated above. The second type consists in larger bcc Li colloids, under much smaller pressure, because they are located in the vicinity of cracks or gas bubbles.

Finally, this picture of spatially separated colloids would also be compatible with the proposed exchange mechanisms, in view of the high concentration of metallic Li in our samples ($\sim 5-10$ at. % as determined by ESR): the distance between colloids becomes smaller than their average size and permits intercolloid exchange. A similar mechanism was proposed by Seinen *et al.*[21] for morphologically varying Na colloids in doped heavily irradiated NaCl.

When the sample is heated the spectra exhibit the transformations shown in Fig. 2. The heating may act in one or more of the following manners: (a) decreasing the correlation time, likely in Arrhenius-type form $\tau_c = \tau_0 \exp(E_a/kT)$, because of self-diffusion of lithium atoms (see, for example, Mali *et al.*[22]); (b) increasing the pressure in the broad (high-ppm) region encapsulated by the matrix; (c) annealing processes; (d) exchange between ''normal'' lithium colloids (narrow component) and ''high-pressure'' ones (broad component); and (e) modification of the possible distribution of the colloid sizes. The latter effect is due to the Knight-shift proportionality to magnetic susceptibility χ, which, in turn, depends on the colloid size N,

$$\chi = \chi_0 \left(1 - \frac{3C}{2} \frac{1}{\sqrt{N}} \right), \tag{2}$$

where χ_0 is the magnetic susceptibility of the bulk metal and C is a constant, according to Engelhardt *et al.*[23] So smaller clusters yield a signal at smaller values of the Knight shift. If, for example, the number of small clusters increases, the resonance line will move towards lower values and may change its form, too (broadening of the spectrum is expected, in general). The above-mentioned factors complicate, therefore, a detailed analysis of the spectra. A useful review on NMR of metal particles and clusters was given by van der Klink and Brom.[24]

Let us first assume that shortening of the correlation times is the dominating mechanism in the behavior of the spectra in Fig. 2. Then, if τ_c is smaller than $1/\nu_r$ and is decreasing with increasing temperature, a narrowing of the line is expected [Eq. (1)]. This behavior is seen for the narrow component (264 ppm) in Fig. 2 in the range from 296 K to about 358 K. When τ_c is larger than $1/\nu_r$ broadening, instead of narrowing, is expected. This seems to be the case of the broader component (271 ppm), for temperatures between 296 K and 327 K. For higher temperatures—358–373 K—this component becomes narrower again and stays well separated from that located near 264 ppm. Such behavior can be understood in terms of τ_c transiting from a region with $\tau_c > 1/\nu_r$ to a region with $\tau_c < 1/\nu_r$.

The behavior of the component located at 264 ppm indicates that, already at 296 K, the correlation time for its nuclei is shorter than $1/\nu_r$. Increasing the temperature until 358 K causes further narrowing due to smaller values of τ_c. At temperatures above 373 K, both components broaden, likely because of an exchange between the two systems.[25] (Below 373 K, the exchange rate between the systems was sufficiently small so that we could observe individual correlation times specific for each system independently.) When the exchange rate increases the lines start to collapse into one broad line. Subsequently, the latter should narrow when the temperature is increasing further. It is just what we observe above 373 K. Another phenomenon notable above 373 K is the shift of the whole spectrum towards lower ppm values. At the highest temperature (436 K) of this run, the high-pressure component (located at 271 ppm at 296 K) vanishes and the remaining spectrum becomes asymmetric with a longer tail at lower ppm values. It could be that changes in the distribution of the colloid sizes have now a bigger influence on the spectrum than the other factors.

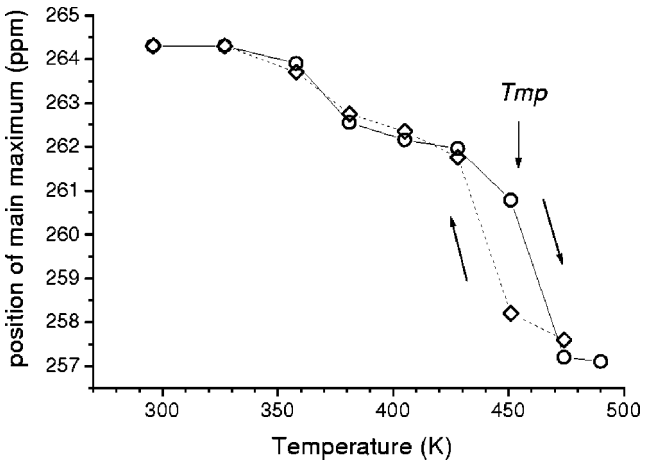

FIG. 5. ^{7}Li MAS NMR in the LD sample. Temperature dependence of the peak position for the narrow line. Circles: increasing T. Diamonds: decreasing T. Note the drop observed at the melting point (T_{mp}) of metallic lithium and the hysteresis upon cooling.

In the subsequent cooling run, the spectra were observed down from 436 K to room temperature. The shapes of the spectra were no longer the same as in the heating run, the main difference being due to changes in the 271-ppm component, which has now transmitted a big part of its intensity to the narrow one.

Even more distinct changes in the NMR spectra were observed in the next runs (Figs. 3 and 4) where the highest temperature (490 K) has crossed the melting point ($T_{mp} = 454$ K) of metallic lithium. Here, again, the two-line structure seems to be lost above 428 K and the remaining single line moves still further toward lower ppm values during heating (Fig. 3); in the cooling run, this single asymmetric line persists down to room temperature (Fig. 4). This single-line feature is also well documented in the inset of Fig. 4, showing the signal recorded with ^{6}Li NMR. If one compares the ^{6}Li MAS NMR spectra presented before the first heating (Fig. 1) and after the last heating run, the loss of the ''high-pressure'' component (at 271 ppm) is remarkable. It is obvious that crossing the lithium melting point is essential for this kind of behavior and is well understood within our model.

Another characteristic aspect of the second heating run is the temperature dependence of the peak positions of the

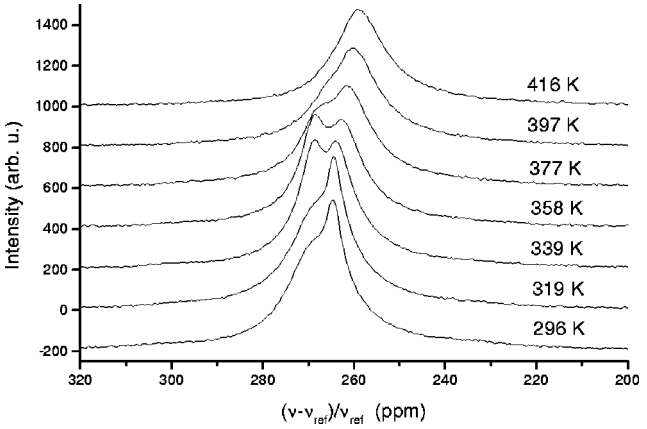

FIG. 6. Evolution of ^{7}Li MAS (5 kHz) NMR spectra in the high-dose irradiated (HD) sample during the first heating run.

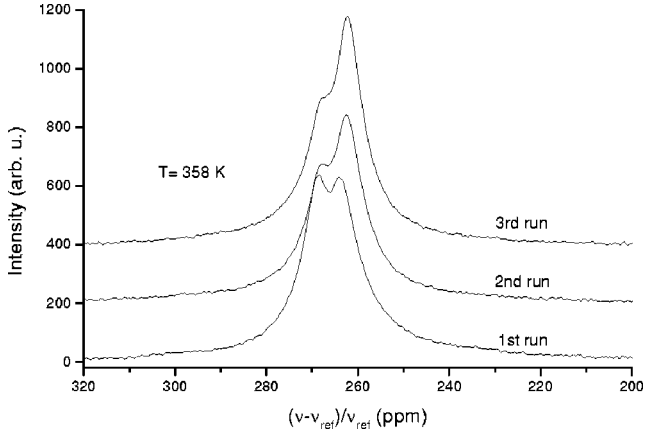

FIG. 7. ^{7}Li MAS (5 kHz) NMR spectra of the HD sample taken at 358 K during three subsequent heating runs, to 416 K, 432 K, and 451 K, respectively.

''normal Li'' line (located at 264 ppm at 296 K) as shown in Fig. 5. Initially, the positions decrease steadily (with a possible minor ''recovery'' stage at 360–370 K) but drop suddenly by ca. 4 ppm after passing 450–460 K—the melting region of metallic lithium. An hysteresis of about 15 K can be noted at T_{mp} between the heating and cooling runs which might be related to a modified stress state in the colloids after melting. Earlier NMR studies[14] do not report any changes in the Knight-shift values at the solid to liquid-state transition for metallic lithium. It may be due to less precise NMR techniques (not MAS) or due to specific characteristics of the employed material (purity, irradiation conditions). Recently, analogous observations of sudden Knight-shift changes during the melting of Na colloids in irradiated NaCl were described by Kanert *et al.* in Ref. 17.

B. High-dose irradiated sample

The ^{7}Li MAS NMR in the twice as much irradiated (HD) sample is shown in Fig. 6. The main difference between the spectra of the LD (Fig. 1) and the HD samples at room temperature is the larger amount of ''high-pressure'' phase in the latter. Considering the shape of its spectrum as a superposition of two Lorentzians the following results are obtained: narrow component (nearly ''bulk'' Li colloids): position 264.3 ppm, linewidth 467 Hz; broad component (''high-pressure''): position 267.2 ppm, linewidth 2514 Hz. The position of the narrow line is the same as found for the LD sample but the width is slightly smaller, which means a somewhat faster motion of Li atoms in the HD sample. Just the opposite is seen for the broad line, since its width is by 60% larger than in the LD sample. Three heating runs have been performed on that sample. In all runs the lowest temperature was 296 K, while the highest were successively 416 K, 432 K, and 451 K. The results of the first heating run shown in Fig. 6 indicate a narrowing of both components between 296 K and 358 K. They start to broaden at 377 K and collapse into a single line at 397 K.

The effect of the three consecutive heat treatments is shown, for example, on the spectrum at $T=358$ K presented in Fig. 7: the spectra are clearly not reproducible. One can see that the narrow, low-ppm, component grows at the expense of the broad one. Moreover, both lines seem to shift towards lower values before coalescing. This could be a signature of increasing exchange rates between both components during subsequent heating events and conversion of part of the high-ppm component into the lower one, together with a stress release at high temperatures.

T_1 experiments by a saturation-recovery technique were made for this sample and the nuclear magnetization decay was found strongly nonexponential. Moreover, it could be decomposed into two different T_1 values. Even if these measurements have a preliminary character, the observation of two relaxation times is coherent with the existence of two types of metallic colloids.

Electron spin resonance experiments conducted in parallel on the above specimens exhibit clear steps near 450 K in the temperature dependence of the CESR linewidths and intensities (somewhat less marked for the HD sample), with strong asymmetry between the heating and cooling runs, thus supporting the present NMR data and their interpretation.

IV. CONCLUSIONS

The present work shows the complex dynamics of lithium atoms in metallic colloids formed by electron irradiation at 50 °C in LiF crystals. A double structure of the Knight-shifted ^{7}Li and ^{6}Li MAS NMR spectra taken at room temperature indicates the presence of two different Li atom environments. In one of them, at higher ppm values, the positions and the linewidths correspond to metallic lithium under pressures much higher than atmospheric. In the second, the values of the above parameters are close to those of metallic Li under normal conditions. (The contribution of the first component to the total intensity is larger for the stronger irradiated HD sample.) Upon heating above 300 K, the correlation time characterizing the nuclear magnetic field fluctuations due to Li atom diffusion shortens first, and that rather independently, in both systems. Above 373 K, however, mutual exchange becomes significant as is demon-

- strated by a broadening of their resonance lines. Simultaneously, some conversion of ''high-pressure'' lithium to ''bulk'' (or ''normal'') one takes place. This is evident when comparing the spectra after consecutive heating runs, in particular when crossing the melting point of metallic lithium. In addition, the whole Knight-shifted spectrum moves towards lower ppm values with increasing temperature, with a jump of nearly 4 ppm when crossing the melting point.

ACKNOWLEDGMENTS

This work was supported by European Community EEC ARI Contract No. HPRI-CT-1999-00042.

*Electronic address: zogal@int.pan.wroc.pl

[1] F. Beuneu and P. Vajda, Phys. Rev. Lett. **76**, 4544 (1996).
[2] F. Beuneu, P. Vajda, G. Jaskierowicz, and M. Lafleurielle, Phys. Rev. B **55**, 11 263 (1997).
[3] C.D. Knutson, H.O. Hooper, and P.J. Bray, J. Phys. Chem. Solids **27**, 147 (1966).
[4] J. Charvolin, J.P. Cohen-Addad, and C. Froidevaux, Solid State Commun. **5**, 357 (1967).
[5] J. Charvolin, C. Froidevaux, C. Taupin, and J.M. Winter, Solid State Commun. **4**, 357 (1966).
[6] F. Beuneu, P. Vajda, and O.J. Żogal, Colloids Surf., A **158**, 83 (1999).
[7] F. Beuneu, P. Vajda, O.J. Żogal, D. Massiot, J.P. Coutures, and P. Florian, Nucl. Instrum. Methods Phys. Res. B **166-167**, 270 (2000).
[8] F. Beuneu and P. Vajda, Radiat. Eff. Defects Solids **150**, 141 (1999).
[9] N.G. Politov and L.F. Vorozheikina, Sov. Phys. Solid State **12**, 277 (1970).
[10] A.T. Davidson, J.D. Comins, T.E. Derry, and F.S. Khumalo, Radiat. Eff. **98**, 305 (1986).
[11] *NMR Spectroscopy Techniques*, edited by C. Dybowski and R.L. Lichter (Dekker, New York, 1987).
[12] T. Takashi, H. Kawashima, H. Sugisawa, and T. Baba, Solid State Nucl. Magn. Reson. **15**, 119 (1999).
[13] J.H. Van Vleck, Phys. Rev. **74**, 1168 (1948).
[14] G.C. Carter, L.H. Bennet, and D.J. Kahan, *Progress in Materials Science* (Pergamon Press, Oxford, 1977), Vol. 20.
[15] H.S. Gutowsky and B.R. McGarvey, J. Chem. Phys. **20**, 1472 (1952); D.F. Holcomb and R.E. Norberg, Phys. Rev. **98**, 1074 (1955).
[16] G. Engelhardt and D. Michel, *High-Resolution Solid-State NMR of Silicates and Zeolites* (Wiley, Chichester, 1987), p. 55; D. Suwelack, W.P. Rothwell, and J.S. Waugh, J. Chem. Phys. **73**, 2559 (1980).
[17] O. Kanert, C. Schmidt, R. Küchler, and H.W. den Hartog, Ber. Bunsenges. Phys. Chem. **101**, 1286 (1997).
[18] R. Bertani, M. Mali, J. Roos, and D. Brinkmann, J. Phys.: Condens. Matter **2**, 7911 (1990).
[19] M. Lambert and A. Guinier, C. R. Hebd. Seances Acad. Sci. **246**, 1678 (1958); M. Lambert, Ch. Mazières, and A. Guinier, J. Phys. Chem. Solids **18**, 129 (1961).
[20] C. Trautmann, M. Toulemonde, J.M. Costantini, J.J. Grob, and K. Schwartz, Phys. Rev. B **62**, 13 (2000).
[21] J. Seinen, D.I. Vainshtein, H.C. Datema, and H.W. den Hartog, J. Phys.: Condens. Matter **7**, 705 (1995).
[22] M. Mali, J. Roos, M. Sonderegger, D. Brinkmann, and P. Heitjans, J. Phys. F: Met. Phys. **18**, 403 (1988).
[23] A. Engelhardt, S. Sotier, and J. Kalus, Z. Naturforsch. A **25a**, 1979 (1970).
[24] J.J. van der Klink and H.B. Brom, Prog. Nucl. Magn. Reson. Spectrosc. **36**, 89 (2000).
[25] J. Sandstroem, *Dynamic NMR Spectroscopy* (Academic Press, London, 1982).